

## Effects of Nematic Fluctuations on the Elastic Properties of Iron Arsenide Superconductors

R. M. Fernandes,<sup>1,\*</sup> L. H. VanBebber,<sup>2</sup> S. Bhattacharya,<sup>3</sup> P. Chandra,<sup>4</sup> V. Keppens,<sup>2</sup> D. Mandrus,<sup>2,5</sup>  
M. A. McGuire,<sup>5</sup> B. C. Sales,<sup>5</sup> A. S. Sefat,<sup>5</sup> and J. Schmalian<sup>1</sup>

<sup>1</sup>*Ames Laboratory and Department of Physics and Astronomy, Iowa State University, Ames, Iowa 50011, USA*

<sup>2</sup>*Department of Materials Science and Engineering, University of Tennessee, Knoxville, Tennessee 37996, USA*

<sup>3</sup>*Tata Institute of Fundamental Research, Homi Bhabha Road, Mumbai 400005, India*

*and Cavendish Laboratory, University of Cambridge, Cambridge CB3 0HE, United Kingdom*

<sup>4</sup>*Department of Physics and Astronomy and Center for Emergent Materials, Rutgers University, Piscataway, New Jersey 08855, USA*

<sup>5</sup>*Materials Science and Technology Division, Oak Ridge National Laboratory, Oak Ridge, Tennessee 37831, USA*

(Received 11 November 2009; published 4 October 2010)

We demonstrate that the changes in the elastic properties of the FeAs systems, as seen in our resonant ultrasound spectroscopy data, can be naturally understood in terms of fluctuations of emerging nematic degrees of freedom. Both the softening of the lattice in the normal, tetragonal phase as well as its hardening in the superconducting phase are consistently described by our model. Our results confirm the view that structural order is induced by magnetic fluctuations.

DOI: 10.1103/PhysRevLett.105.157003

PACS numbers: 74.25.Ld, 74.25.Kc, 74.62.Fj, 74.70.-b

In the recently discovered FeAs superconductors [1,2], the rather large superconducting transition temperatures are in close proximity to an antiferromagnetic (AFM) phase transition at  $T_N$  and a structural transition from tetragonal (Tet) to orthorhombic (Ort) at  $T_S$  [3–6]. This begs the question to what extent spin and lattice degrees of freedom play important roles for high- $T_c$  superconductivity (SC). The fact that  $T_S$  and  $T_N$  track each other closely (see inset of Fig. 3), as well as the existence of an isotope effect for  $T_N$  [7], is clear evidence that they signal the onset of strongly coupled ordered states. Since  $T_S \geq T_N$ , it seems, at first glance, plausible to assume that lattice effects are primary and the AFM order is simply a secondary effect. However, it has been suggested [8,9] that spin fluctuations, related to the observed AFM ordering at  $T_N$ , will, at higher temperatures, lead to emergent nematic degrees of freedom [10] that couple to the lattice [11,12]. Even though of magnetic origin, probing nematic fluctuations is nontrivial, since the magnetic field fluctuations associated with them average to zero. Thus, determining to what extent these fluctuations are present is key for identifying the relevant low energy modes in the pnictides.

Recent experiments [13,14] found strong anisotropy in the electronic properties of the Ort phase, suggesting an underlying electronic nematic state. In this Letter, we focus on the Tet phase and demonstrate that the measurement of the shear modulus  $C_s$  allows for a direct determination of the nematic order-parameter susceptibility  $\chi_{\text{nem}}$ . In particular, we show that the high-temperature shear modulus  $C_{s,0}$  is renormalized by nematic fluctuations to

$$C_s^{-1} = C_{s,0}^{-1} + \lambda^2 C_{s,0}^{-2} \chi_{\text{nem}}, \quad (1)$$

where  $\lambda$  is the magnetoelastic coupling. We calculate  $\chi_{\text{nem}}$  in the Tet phase using a  $1/N$  approach and compare the results with resonant ultrasound spectroscopy (RUS),

which measures  $C_s$ . Our RUS data show that nematic fluctuations are prominent over a large portion of the phase diagram of the pnictides. Although driven by AFM fluctuations, they represent new emergent collective degrees of freedom. Their coupling to the lattice makes the structural transition coincident with the nematic transition, implying that the elastic degrees of freedom are secondary with respect to the electronic ones. Here, we analyze the behavior of nematic fluctuations not only in the normal state, but also in the vicinity of  $T_c$ , explaining the observed hardening of  $C_s$  in the SC state.

In the AFM phase, spins are coupled antiferromagnetically for Fe-Fe bonds along one diagonal and ferromagnetically along the other diagonal of the two-Fe unit cell (Fig. 1). The in-plane magnetic ordering can be divided into two sublattices [15] with Néel magnetizations  $\mathbf{m}_1$  and  $\mathbf{m}_2$ , which are weakly coupled since in the classical ground state local fields associated with one sublattice cancel in the other.

This sublattice coupling is related to a  $Z_2$  (i.e., discrete, Ising-type) symmetry:  $\mathbf{m}_1 \rightarrow -\mathbf{m}_1$ ,  $\mathbf{m}_2 \rightarrow \mathbf{m}_2$ , along with a rotation of the coordinates by  $\pi/2$ . The  $Z_2$  symmetry, manifest by the two possible orientations of the magnetic stripes, will give rise to an Ising-like order parameter, which in the continuous limit is given by  $\varphi(x) = \mathbf{m}_1(x) \cdot \mathbf{m}_2(x)$  [10], with  $x = (\mathbf{r}, \tau)$ , as shown in Fig. 1. It describes the relative orientation of  $\mathbf{m}_1$  and  $\mathbf{m}_2$  and does not change sign upon magnetic field inversion. The particular magnetic structure of the pnictides naturally accounts for this emergent degree of freedom, regardless of whether one considers an itinerant [16,17] or a localized [18] picture. Once  $\langle \varphi \rangle \neq 0$ , the  $Z_2$  symmetry is spontaneously broken [10], and so is the underlying  $C_4$  symmetry of the lattice. This is why one associates the Ising-ordered phase to a “nematic” state, even though, strictly speaking, the full

rotational symmetry, as well as the translational symmetry, is already broken above  $T_S$ .

To probe  $\varphi$ , we use the fact that the nematic order couples to the elastic degrees of freedom of the lattice [11,19]: in orthorhombic fluctuations, present for  $T > T_S$ , bonds connecting antiparallel spins are expanded, whereas those connecting parallel spins contract [20,21] (see Fig. 1). There is therefore an energy cost associated with such an orthorhombic fluctuation, characterized by the shear modulus  $C_s \equiv C_{66}$ . Shear strain ( $\epsilon_s = 2\epsilon_{xy}$ , where  $\epsilon_{\alpha\beta}$  is the strain tensor) and the nematic order parameter are linearly coupled in the energy:

$$S_{\text{el-mag}} = \lambda \int_x \epsilon_s(x) \varphi(x); \quad (2)$$

i.e., they order simultaneously. Here  $\lambda > 0$  is the magnetoelastic coupling constant and  $\int_x \dots = \int_0^{T^{-1}} d\tau \int d^3r \dots$ . Assuming a harmonic lattice for  $\lambda = 0$ , with bare (high-temperature) shear modulus  $C_{s,0}$ , we obtain the renormalized  $C_s$  in Eq. (1). Note that the static nematic susceptibility  $\chi_{\text{nem}} = \chi_{\text{nem}}(q \rightarrow 0)$  is a four-spin correlation function, given by  $\chi_{\text{nem}}(q) = \langle \varphi_q \varphi_{-q} \rangle - \langle \varphi_q \rangle^2$ , where  $\varphi_q$  denotes the Fourier transform of  $\varphi(x)$ . From Eq. (1), we see that nematic fluctuations soften the lattice in the Tet phase ( $T > T_S$ ). A divergence of  $\chi_{\text{nem}}$  brings  $C_s$  to zero, signaling the onset of the Tet-Ort transition.

To probe the shear modulus in the pnictides, RUS [22] was performed on undoped  $\text{BaFe}_2\text{As}_2$  and optimally doped  $\text{BaFe}_{1.84}\text{Co}_{0.16}\text{As}_2$  single crystals grown out of FeAs flux [23]. More than 20 mechanical resonance frequencies  $f$

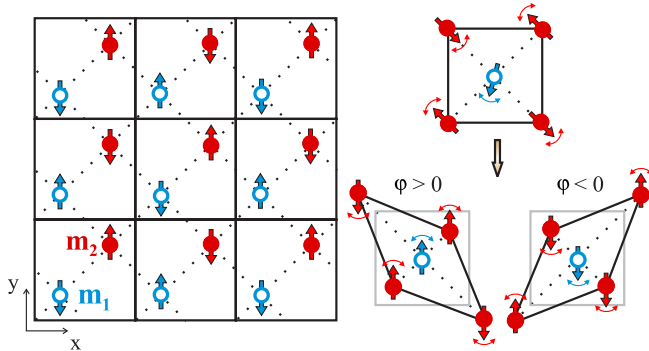


FIG. 1 (color online). Left-hand panel: In-plane magnetic ordering of the pnictides. The two iron atoms present in one tetragonal unit cell (open blue circles and filled red circles) form two coupled AFM sublattices with coplanar staggered magnetization  $\mathbf{m}_1$  and  $\mathbf{m}_2$ . Right-hand panel: In the disordered phase, the spins in the two sublattices fluctuate around two arbitrary staggered magnetization directions. In the nematic phase, these two Néel vectors are locked either parallel ( $\varphi > 0$ ) or antiparallel ( $\varphi < 0$ ) to each other, but still with  $\langle \mathbf{m}_1 \rangle = \langle \mathbf{m}_2 \rangle = 0$ . The coupling between the nematic and the elastic order parameters makes the bonds between neighboring parallel (antiparallel) spins contract (expand).

were detected. Since the crystals have 6 independent elastic constants  $C_{ij}$  in the Tet phase, it is clear that each resonance line  $f$  will be proportional to a combination of  $C_{ij}$ . Extraction of the full elastic tensor is not possible due to samples size limitations, but information about  $C_s = C_{66}$  can be obtained. Because the samples undergo a Tet-Ort transition,  $C_s$  must get soft by symmetry. Numerical simulations of the resonance spectrum show that this soft  $C_s$  dominates several of the measured lines, with  $f^2 \propto C_s$  [22].

Following this procedure we present (Fig. 2) the  $T$  dependence of two resonance frequencies that are representative of a larger set of  $C_s$ -dominated lines. The observed reduction in  $f^2$  indicates a dramatic softening of  $C_s$ . In the undoped case [Fig. 2(a)], this softening is cut off by a simultaneous structural-AFM weak first order transition at  $T_S = 130$  K. In the optimally doped case [Fig. 2(b)], where no AFM or structural transitions are present, the softening continues to lower temperatures until it is truncated by the SC transition at  $T_c = 22$  K. In order to

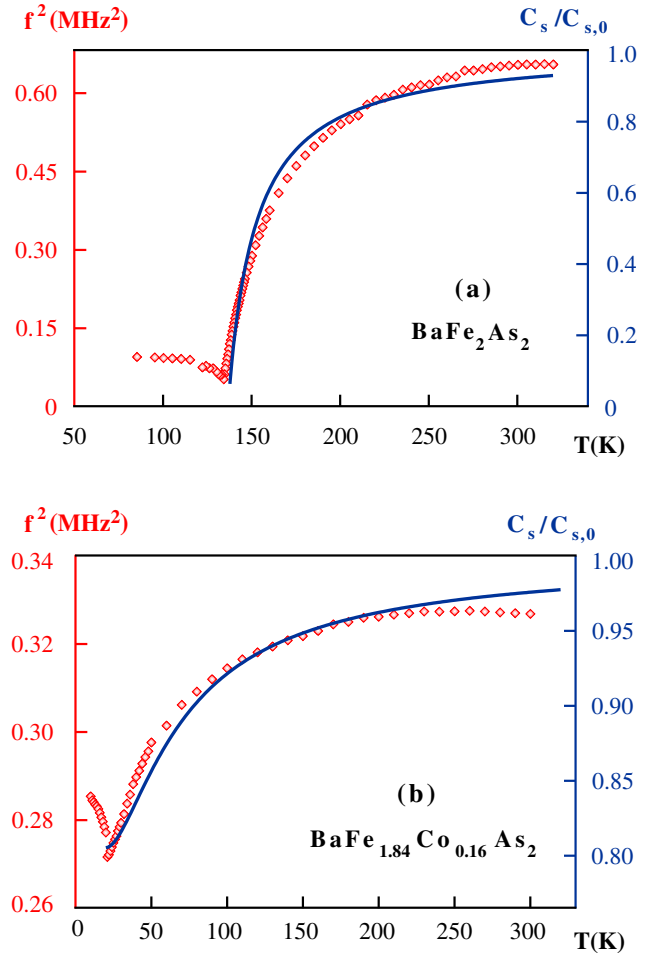


FIG. 2 (color online). Temperature dependence of the RUS measured squared resonant frequency  $f^2$  (red points), and of the calculated shear modulus  $C_s \equiv C_{66}$  of the tetragonal phase (solid blue line), for both (a) undoped  $\text{BaFe}_2\text{As}_2$  and (b) optimally doped  $\text{BaFe}_{1.84}\text{Co}_{0.16}\text{As}_2$ .

confirm that these features are not due to any particular mechanical instability of the samples, we also performed RUS in strongly doped samples that present neither SC nor structural transitions. In this case, only a uniform, mild increase in  $f$  with decreasing  $T$  was observed.

Next, we calculate the nematic susceptibility  $\chi_{\text{nem}}$  in Eq. (1). Following Refs. [8,9] we introduce an action  $S = S_{\text{mag}} + S_{\text{el}} + S_{\text{el-mag}}$  for the magnetic and elastic degrees of freedom, with  $S_{\text{el-mag}}$  given by Eq. (2). For each sublattice in Fig. 1, we consider

$$S_{\text{mag}}^{(0)}[\mathbf{m}_i] = \frac{1}{2} \int_q \tilde{\chi}_{0,q}^{-1} |\mathbf{m}_i(q)|^2 + \frac{w}{4} \int_x \mathbf{m}_i^4(x), \quad (3)$$

where  $w > 0$  is a coupling constant and  $q = (\mathbf{q}, i\omega_n)$  refers to momentum  $\mathbf{q}$ , measured relative to the ordering vector  $\mathbf{Q} = (\frac{\pi}{a}, \pm \frac{\pi}{a})$ , and bosonic Matsubara frequency  $\omega_n$ , with  $\int_q \cdots = T \sum_n \int \frac{d^3q}{(2\pi)^3} \cdots$ . The bare spin susceptibility  $\tilde{\chi}_{0,q}$  is assumed to be  $\tilde{\chi}_{0,q}^{-1} = r_0 + \mathbf{q}_{\parallel}^2 - 2J_z \cos(q_z c) + \Pi(\omega_n)$ . Here, the particle-hole bubble  $\Pi(\omega_n)$  is determined by the electronic structure and leads to a sensitivity of  $\tilde{\chi}_{0,q}$  with respect to SC. Not only the static part of  $\tilde{\chi}_{0,q}$  is changed in the SC state, but also its dynamics [24]: the opening of the SC gap  $\Delta$  makes the spin dynamics ballistic for  $\omega_n \ll \Delta$  ( $z = 1$ ), while for  $\omega_n \gg \Delta$  one recovers the overdamped dynamics of a metallic AFM ( $z = 2$ ). Thus, we can write  $\Pi(\omega_n) - \Pi(0) = \Gamma_z |\omega_n|^{2/z}$  with Landau particle-hole damping coefficient  $\Gamma_{z=2} = \gamma^{-1}$  as well as  $\Gamma_{z=1} \simeq (\Delta\gamma)^{-1}$ .  $r_0$  characterizes the distance to a magnetic critical point and  $J_z$  is a magnetic coupling between Fe-As layers separated by  $c$ . To describe systems of different Co doping, we vary  $\gamma$  and  $r_0$ . The full magnetic action is given by the sum of the contributions of the two sublattices and the dominant [9,11] term that couples them:

$$S_{\text{mag}} = \sum_i S_{\text{mag}}^{(0)}[\mathbf{m}_i] - \frac{g}{2} \int_x (\mathbf{m}_1(x) \cdot \mathbf{m}_2(x))^2, \quad (4)$$

where  $g > 0$  is the sublattice coupling. In a localized picture,  $g$  is related to quantum and thermal spin fluctuations [10], whereas in an itinerant picture it is related to the ellipticity of the electron band [16,25]. To solve for the coupled magnetic and elastic system we assume that  $\mathbf{m}_i$  is an  $N$ -component vector and analyze the leading term for large- $N$  [8,9]. We find

$$\chi_{\text{nem}}(q) = \frac{\chi_{0,\text{nem}}(q)}{1 - g_r \chi_{0,\text{nem}}(q)}, \quad (5)$$

where  $g_r = g + \lambda^2/C_{s,0}$  is the sublattice coupling renormalized by magnetoelastic interactions. Thus, even if  $g = 0$ , the magnetoelastic coupling gives an effective coupling between the sublattices.  $\chi_{0,\text{nem}}(q) = N \int_p \tilde{\chi}_p \tilde{\chi}_{p+q}$  is determined by the dynamic magnetic susceptibility  $\tilde{\chi}_p$  of Eq. (3) but with  $r_0 + \Pi(0)$  replaced by  $r = \xi^{-2}$ .  $\xi$  is the magnetic correlation length, determined in the large  $N$  approach. If  $d + z \leq 4$  it follows that  $\chi_{0,\text{nem}}(0)$  diverges

as  $\xi \rightarrow \infty$ . Here, the system has  $d = 2$  ( $d = 3$ ) behavior for  $r \gg J_z$  ( $r \ll J_z$ ). Thus, a sufficiently large, but finite  $\xi$  suffices to cause a divergence of  $\chi_{\text{nem}}$ , implying that the Tet-Ort transition is induced by AFM fluctuations, not AFM order; hence,  $T_S > T_N$  (except when at least one of the transitions is first order).

First, we present our results for the Tet and non-SC state in Fig. 2, together with the RUS data. The spin dynamics is overdamped (i.e.,  $z = 2$ ), as seen in inelastic neutron scattering [26]. We used the parameters  $\gamma_{\text{undoped}}^{-1} = 2.2 \times 10^{-3}$ ,  $\gamma_{\text{doped}}^{-1} = 4.7 \times 10^{-3}$ ,  $g = 0.015\epsilon_0$ ,  $\frac{\lambda^2}{C_{s,0}} = 10^{-3}\epsilon_0$ , and  $J_z = 10^{-3}\epsilon_0$ , where  $\epsilon_0 \approx 3.4$  meV is a magnetic energy scale. The value for the Landau damping is consistent with that used in Ref. [26]. The lattice softening, seen in the experiment over a large temperature range, can be well described by the above theory, suggesting nematic fluctuations up to room temperature and over a significant portion of the phase diagram. The amplitude of the effect indicates a strong magnetoelastic coupling, consistent with the observed softening of some phonon frequencies [27].

For both samples, the lattice softening in the RUS data stops at low  $T$ . For zero doping this happens at the joint first order structural-AFM transition, where a hardening of the lattice is expected. Because of the Fermi surface reconstruction in the AFM phase, however, a quantitative description of  $C_s$  below  $T_N$  is beyond the scope of our model.

For optimal doping, the lattice also gets harder below  $T_c$ . In this case, though, there is *a priori* no reason for  $C_s$  to be minimum at  $T_c$ . Note that this behavior is distinct from the Testardi behavior seen in other superconductors, where strain couples to the squared SC order parameter  $|\Psi|^2$ , and changes the transition temperature  $T_c \rightarrow T_c(\epsilon_{ab})$ , making the elastic modulus behave very similarly to minus the heat capacity at the transition [28,29]. Here, symmetry prohibits such a coupling and non-Testardi behavior is expected at  $T_c$ .

To understand our results close to  $T_c$  we determine the dynamic spin response in the normal and SC phase. Analyzing the spin dynamics, ballistic for  $\omega \ll \Delta$  and overdamped for  $\omega \gg \Delta$ , we find that the frequency integral in  $\chi_{0,\text{nem}}$  is dominated by overdamped dynamics ( $z = 2$ ). Therefore, the key impact of the SC phase is not on the dynamics, but on the static part of the susceptibility. Magnetism in the pnictides has been shown to be strongly affected by SC, to the extent that the AFM order parameter is suppressed below  $T_c$  [30,31]. A Landau expansion for the competition of the AFM and SC order parameter is governed by the coupling  $\frac{\lambda_m}{2} |\Psi(x)|^2 [\mathbf{m}_1^2(x) + \mathbf{m}_2^2(x)]$  [32,33]. Close to  $T_c$  this coupling leads to an increase in the inverse magnetic correlation length  $r \rightarrow r + \lambda_m \langle |\Psi(x)|^2 \rangle$ , which suppresses the static part of the spin susceptibility  $\tilde{\chi}_p$ . Thus, magnetic order and correlations are weakened in the SC state and  $\chi_{0,\text{nem}}(0) = N \int_p \tilde{\chi}_p^2$  acquires a minimum at  $T_c$ . Given the overdamped spin dynamics we obtain  $\chi_{0,\text{nem}}(0) \propto -\ln(r + \lambda_m \langle |\Psi|^2 \rangle)$  for

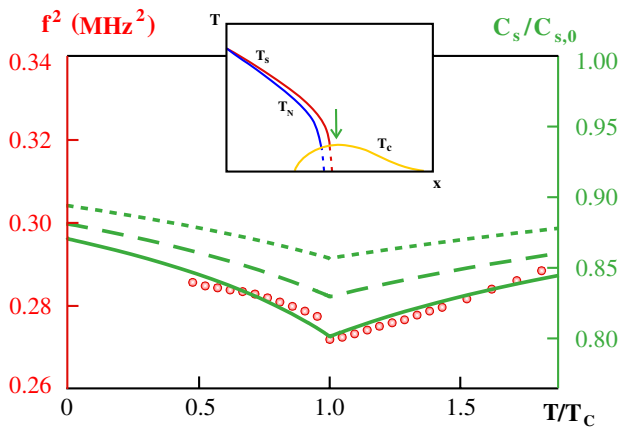


FIG. 3 (color online). Shear modulus  $C_s$  in the tetragonal, SC phase. The inset shows a schematic  $(x, T)$  phase diagram for  $\text{Ba}(\text{Fe}_{1-x}\text{Co}_x)_2\text{As}_2$ , with the green arrow denoting optimal doping. In the main panel, the solid line refers to the optimally doped system, whereas the dashed and dotted curves refer to systems that are, respectively, deeper in the overdoped region. The red points refer to the RUS data of Fig. 2(b).

2D magnetic fluctuations. To show that this effect explains the observed anomaly of  $C_s$  at  $T_c$ , we compare in Fig. 3 the RUS data for the optimally doped sample with our theory. In general, the correction to  $\xi^{-2}$  is proportional to the composite operator  $\langle |\Psi|^2 \rangle \propto (T_c - T)^{1-\alpha}$ , yet the SC transition is well described by a mean-field approach ( $\alpha = 0$ ). On general grounds, one expects the AFM fluctuations to get weaker along the overdoped region, which would lead to a less pronounced softening of the lattice for  $T > T_c$ .

We note that the reduction of  $C_s$  close to the Tet-Ort transition is a general feature, expected in any critical theory. However, the hardening of the lattice below  $T_c$ , where there is no structural instability, is an unexpected observation. Yet, it finds a natural explanation in terms of magnetically driven nematic fluctuations and competing AFM and SC order. Furthermore, the same model is able to explain the reduction of orthorhombic (i.e., nematic) order in the SC state, as observed in Ref. [34]. The existence of nematic fluctuations is crucial to our results: if one considered only generic magnetic fluctuations, the relevant magnetoelastic coupling would be  $\mathbf{m}^2 \varepsilon_{ii}$ , instead of Eq. (2). In this case, the magnetization would couple not to the shear distortion, but to the longitudinal modes, which cannot explain the strong correlation between the AFM and the Tet-Ort transitions.

In summary, the spin ordering in the pnictides results in emergent nematic degrees of freedom that can be probed through the shear modulus. Our results show that both magnetic and nematic or, equivalently, shear degrees of freedom are important low energy excitations in a large temperature and doping regime of the system.

We thank S. Bud'ko, P. Canfield, A. Goldman, A. Kreyssig, and R. McQueeney for fruitful discussions.

Work at Ames Laboratory and ORNL was supported by the U.S. DOE, Office of Basic Energy Sciences, Materials Science and Engineering Division. L.H.V. and V.K. (NSF-DMR-0804719) and P.C. (NSF-NIRT-ECS-0608842) thank the NSF for financial support. The authors acknowledge the hospitality of the Aspen Center for Physics (J.S. and P.C.) and of the Trinity College, University of Cambridge (S.B.).

\*rafaelfm@ameslab.gov

- [1] Y. Kamihara *et al.*, *J. Am. Chem. Soc.* **130**, 3296 (2008).
- [2] M. Rotter, M. Tegel, and D. Johrendt, *Phys. Rev. Lett.* **101**, 107006 (2008).
- [3] H. Luetkens *et al.*, *Nature Mater.* **8**, 305 (2009).
- [4] N. Ni *et al.*, *Phys. Rev. B* **78**, 214515 (2008).
- [5] J.-H. Chu *et al.*, *Phys. Rev. B* **79**, 014506 (2009).
- [6] F. Ning *et al.*, *J. Phys. Soc. Jpn.* **78**, 013711 (2009).
- [7] R.H. Liu *et al.*, *Nature (London)* **459**, 64 (2009).
- [8] C. Fang *et al.*, *Phys. Rev. B* **77**, 224509 (2008).
- [9] C. Xu, M. Müller, and S. Sachdev, *Phys. Rev. B* **78**, 020501(R) (2008).
- [10] P. Chandra, P. Coleman, and A. I. Larkin, *Phys. Rev. Lett.* **64**, 88 (1990).
- [11] Y. Qi and C. Xu, *Phys. Rev. B* **80**, 094402 (2009).
- [12] V. Barzykin and L.P. Gor'kov, *Phys. Rev. B* **79**, 134510 (2009).
- [13] T.-M. Chuang *et al.*, *Science* **327**, 181 (2010).
- [14] J.-H. Chu *et al.*, *Science* **329**, 824 (2010).
- [15] T. Yildirim, *Phys. Rev. Lett.* **101**, 057010 (2008).
- [16] I. Eremin and A. V. Chubukov, *Phys. Rev. B* **81**, 024511 (2010).
- [17] I. I. Mazin and J. Schmalian, *Physica (Amsterdam)* **469C**, 614 (2009).
- [18] Q. Si and E. Abrahams, *Phys. Rev. Lett.* **101**, 076401 (2008).
- [19] C. Fang *et al.*, *Phys. Rev. B* **74**, 094508 (2006).
- [20] J. Zhao *et al.*, *Phys. Rev. B* **78**, 140504 (2008).
- [21] A. Jesche *et al.*, *Phys. Rev. B* **78**, 180504 (2008).
- [22] A. Migliori and J.D. Maynard, *Rev. Sci. Instrum.* **76**, 121301 (2005).
- [23] A. S. Sefat *et al.*, *Phys. Rev. Lett.* **101**, 117004 (2008).
- [24] Ar. Abanov and A. V. Chubukov, *Phys. Rev. Lett.* **83**, 1652 (1999).
- [25] J. J. Pulikotil *et al.*, *Supercond. Sci. Technol.* **23**, 054012 (2010).
- [26] D. S. Inosov *et al.*, *Nature Phys.* **6**, 178 (2010).
- [27] R. Mittal *et al.*, *Phys. Rev. Lett.* **102**, 217001 (2009).
- [28] A. J. Millis and K. M. Rabe, *Phys. Rev. B* **38**, 8908 (1988).
- [29] J. Nyhus *et al.*, *Physica (Amsterdam)* **369C**, 273 (2002).
- [30] D.K. Pratt *et al.*, *Phys. Rev. Lett.* **103**, 087001 (2009).
- [31] A.D. Christianson *et al.*, *Phys. Rev. Lett.* **103**, 087002 (2009).
- [32] S. Sachdev and E. Demler, *Phys. Rev. B* **69**, 144504 (2004).
- [33] R.M. Fernandes *et al.*, *Phys. Rev. B* **81**, 140501(R) (2010).
- [34] S. Nandi *et al.*, *Phys. Rev. Lett.* **104**, 057006 (2010).